Modeling of Microstructures in a Cosserat Continuum Using Relaxed Energies

Muhammad Sabeel Khan and Klaus Hackl

Abstract Granular materials tend to exhibit distinct patterns under deformation consisting of layers of counter-rotating particles. In this article, we are going to model this phenomenon on a continuum level by employing the calculus of variations, specifically the concept of energy relaxation. In the framework of Cosserat continuum theory the free energy of the material is enriched with an interaction energy potential taking into account the counter rotations of the particles. The total energy thus becomes non-quasiconvex, giving rise to the development of microstructures. Relaxation theory is then applied to compute its exact quasiconvex envelope. It is worth mentioning that there are no further assumptions necessary here. The computed relaxed energy yields all possible displacement and micro-rotation field fluctuations as minimizers. Based on a two-field variational principle the constitutive response of the material is derived. Results from numerical computations demonstrating the properties of relaxed potential are shown.

1 Introduction

This paper focuses on the treatment of a non-quasiconvex, and therefore ill-posed variational model for granular materials that arises as a consequence of the particle counter rotations at the microscale. In continuum mechanics non-quasiconvex potentials may arise due to various reasons, e.g., in the case of strain-softening plasticity [34, 40] they can be caused by non-monotone constitutive behavior, in the case of single slip plasticity they can be due to single slip constraints on the deformation of crystal in association with cross-hardening [23, 24], for twinning induced plasticity they stem from multi-phase energy potentials corresponding to different martensitic variants [8, 14, 32, 35, 36].

M. Sabeel Khan · K. Hackl (✉)
Lehrstuhl für Mechanik-Materialtheorie, Ruhr-Universität, Bochum, Germany
e-mail: klaus.hackl@rub.de

E. Rocca et al. (eds.), *Trends in Applications of Mathematics to Mechanics*,
Springer INdAM Series 27, https://doi.org/10.1007/978-3-319-75940-1_6

So far, different approaches have been discussed in the literature to treat non-quasiconvex variational problems. One possibility is to use regularization techniques which are based on a gradient-type enhancement of the original non-quasiconvex energy function in (5). But the regularization method has its own limitations as far as the physical properties of the unrelaxed problems are concerned.

Contrary to this is the method of relaxation is a more effective and natural way to deal with non-quasiconvex energies. There are two ways to relax the original non-quasiconvex energy minimization problem (5). Either to enlarge the space of admissible deformations $\left(W^{1,p\in(1,\infty)}(\Omega,\mathbb{R}^n)\right)$ to the space of parametrized measures [8, 47, 64], or, to replace the original non-quasiconvex energy with its relaxed energy envelope. The methodology of constructing a relaxed minimization problem by using parametrized measures is discussed by Carstensen and Roubíček [15, 16], Nicolaides and Walkington [42, 43], Pedregal [47–49] and Roubíček [51–53]. The references which suggests to replace the non-quasiconvex energy with its corresponding relaxed energy function are found in Carstensen et al. [13], Conti and Ortiz [23], Conti and Theil [24], Hackl and Heinen [35], Govindjee et al. [32], Miehe and Gürses [34]. Numerical schemes for calculating relaxed envelopes have been worked out by Aranda and Pedregal [4], Bartels [10], Carstensen, Conti and Orlando [12], Carstensen and Plechac [14], Carstensen and Roubíček [15], Chipot [19], Chipot and Collins [20], Collins, Kinderlehrer and Luskin [21], Dolzmann and Walkington [29], Pedregal [49] and Roubíček [53]. For a detailed discussion on the methods of relaxation the reader is referred to the work by Dacorogna [25], Ball [7] and references therein.

Exact analytical results for the relaxed energy are known only for few variational problems in the literature so far. For example the work of DeSimone and Dolzmann [28] where they give an exact envelope of the relaxed energy potential for the free energy of the nematic elastomers undergoing a transition from isotropic to nematic-phase. Dret and Raoult [30] compute an exact quasiconvex envelope for the Saint Venant-Kirchhoff stored energy function expressed in terms of singular values. Some analytical examples of quasiconvex envelopes are also mentioned by Raoult in [50] for different models in nonlinear elasticity. Kohn and Strang [37, 38] gave an exact formula (see Theorem 1.1 in [37]) for the relaxed energy for a variational problem which has its emergence from the shape optimization problems for electrical conduction. Another exact relaxed result is given by Conti and Theil in [24] for the incremental variational problem for rate-independent single slip elastoplasticity. Conti and Ortiz [23] determine an exact analytical expression for the relaxed energy in single crystal plasticity with a non-convex constraint on the deformation of the crystal requiring all material points must deform via single slip. They extended their analytical expression in [22] to the case of crystal plasticity with arbitrary hardening features. Kohn and Vogelius studied the inverse problem of applied potential tomography and come up with an analytical formula [39] for the relaxed energy by using results from homogenization. In a similar manner but this time with the use of Fourier analysis Kohn presents in Theorem 3.1 of [36] an exact analytical expression for a two well energy function with application to solid-solid phase transitions.

In this paper, we provide an exact relaxation for the non-quasiconvex energy which arises during our study on the rotational microstructures in granular materials. Due to a large number of industrial applications and their use in everyday life granular materials have been studied extensively throughout the past years. Numerous investigations have been performed in order to model the mechanical behavior of these materials [2, 3, 18, 31, 44–46, 54–57, 59, 60]. In this work, the focus is to consider the counter-rotations of granular particles at the microscale and to develop a mechanical model that can predict the formation of distinct deformation patterns that are related to the microstructures in these materials. For an overview on the experimental observations of such patterns the reader is referred to the book by Aranson and Tsimring [5]. For this purpose the continuum description of granular materials is used, specifically the theory of Cosserat continuum.

The present work is organized as follows. In Sect. 2 the intergranular kinematics is discussed and an interaction energy potential contributing to the strain energy of the material is proposed. In Sect. 3 a relaxed variational model for granular materials is presented where we state and prove a theorem on the explicit computation of the relaxed envelope. Employing this result, the exact relaxed energy is derived where all the material regimes are explicitly characterized. In Sect. 4 numerical results demonstrating on the properties of computed relaxed potential are presented. Finally in Sect. 5 conclusions are drawn.

2 Intergranular Interactions and Counter Rotations

Intergranular interactions and particle counter rotations in a granular medium subjected to deformation are intriguing and experimentally well recognized [44, 54] phenomenon that contribute in the development of material microstructures [9, 55, 58]. Because of intricate nature of particle rotations and complex behavior of granular materials under deformation it is therefore difficult to understand the intergranular cohesive interactions completely. In literature almost no comprehensive study appeals which discuss the intergranular interactions and the arising phenomenon in detail that can truly justify the naturally observed microstructural patterns in deforming granular materials. Although the particle rotations at the microscale has been considered by a number of authors, see e.g. [1, 17, 18, 45, 55, 58], the essence of their counter rotations especially their interactions in observing the formation of distinct deformation patterns is not well understood. It is therefore our aim to reconsider the intergranular kinematics of counter-rotating particles at microscale and to develop an interaction energy potential for a granular medium that arises as a consequence of these particle counter rotations.

Here, we develop an interaction energy potential that takes into account the intergranular kinematics at the continuum scale and define two new material parameters as a suitable measure for the observation of microstructural phases of granular materials. In this spirit, consider the granular material where two neighboring particles are in contact with each other as shown in Fig. 1. These particle interactions

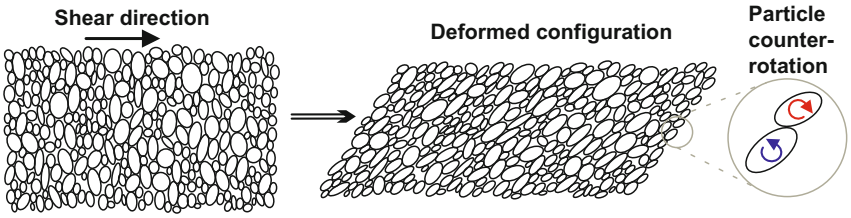

Fig. 1 Schematic of a granular medium subjected to shear with phenomenon of particle counter rotations

leads to two important modes of deformations called translational and micro-rotational motions of the particles which can play a crucial role in the dissipation of the material energy [1, 45] at the continuum scale and therefore contribute to the material strain energy. These independent translational and rotational motions of the granules at the microscale are interlinked with a suitable deformation measure analogous to the concept used in the theory of generalized continuum. Consider now that at the continuum scale the translational motion of the two interacting particles is represented by the vector field $\{u_i\,\mathbf{e}_i\} : \mathbb{R}^d \mapsto \mathbb{R}^d$ and the rotational motion is represented by a field vector analogous to the micro-rotational vector $\{\varphi_i\,\mathbf{e}_i\} : \mathbb{R}^d \mapsto \mathbb{R}^d$ of the Cosserat continuum. Associated with these deformation field vectors are the strain measures. Corresponding to translational and microrotational vector field these measure are the deformation tensor $\left[u_{j,i}\,\mathbf{e}_i \otimes \mathbf{e}_j\right] : \mathbb{R}^d \mapsto \mathbb{R}^{d\times d}$ and $\left[\varphi_{j,i}\,\mathbf{e}_i \otimes \mathbf{e}_j\right] : \mathbb{R}^d \mapsto \mathbb{R}^{d\times d}$ respectively. The symmetric part of $u_{j,i}\,\mathbf{e}_i \otimes \mathbf{e}_j$ is the classical strain tensor $\varepsilon_{ij}\,\mathbf{e}_i \otimes \mathbf{e}_j$. An investigation of the rotating phenomenon of the interacting particles reveals that the macroscopic shear $\left(\varepsilon_{ij} - \dfrac{1}{d}\varepsilon_{kk}\,\delta_{ij}\right)\mathbf{e}_i \otimes \mathbf{e}_j$ influence the microrotational deformation $\varphi_{j,i}\,\mathbf{e}_i \otimes \mathbf{e}_j$ of the granular particles. This leads us to suggest a proportionality relation between the gradient of the microrotational vector field and the macroscopic shear strain which in mathematical terms is given by

$$\sqrt{\sum_{i,j=1}^{d}\left(\varphi_{j,i}\right)^2} \propto \sqrt{\sum_{i,j=1}^{d}\left(\varepsilon_{ij} - \frac{1}{d}\varepsilon_{kk}\,\delta_{ij}\right)^2}, \tag{1}$$

where d is the dimension of the problem under consideration. This proportionality relation is solved with the introduction of the length scale parameter β with the dimension of the inverse of a length. Thus we can write

$$\sqrt{\sum_{i,j=1}^{d}\left(\varphi_{j,i}\right)^2} = \beta \sqrt{\sum_{i,j=1}^{d}\left(\varepsilon_{ij} - \frac{1}{d}\varepsilon_{kk}\,\delta_{ij}\right)^2}. \tag{2}$$

Equation (2) is indeed the simplest possible assumption taking into account such an intergranular relationship. More complex forms can be envisioned, but we will demonstrate in the sequel that the present one already leads to a very intricate kinetics.

This brief but comprehensive discussion on itergranular kinematics enables us to propose an interaction energy potential that will contribute to the material strain energy function. This interaction energy potential is stated as

$$\mathscr{I} = \alpha \left(\sum_{i,j=1}^{d} \left(\varphi_{j,i}\right)^2 - \beta^2 \sum_{i,j=1}^{d} \left(\varepsilon_{ij} - \frac{1}{d} \varepsilon_{kk}\, \delta_{ij} \right)^2 \right)^2 , \tag{3}$$

where Einstines summation convention is assumed. In tensorial notation it takes the following form

$$\mathscr{I} \;=\; \alpha \left(\|\nabla \boldsymbol{\varphi}\|^2 - \beta^2 \, \|\mathrm{sym}\, \mathrm{dev}\, \nabla \mathbf{u}\|^2 \right)^2 , \tag{4}$$

where α and β are non-negative material constants, α is the interaction modulus having information regarding frictional effect in the interacting particles and β is related to the particle size having information regarding intrinsic length scale in Cosserat continuum. The proposed interaction energy potential not only bridges the gap between microstructural properties and the macroscopic behavior of the material but also enables us to characterize different microstructural regimes in granular materials.

3 A Relaxed Variational Model for Granular Materials

3.1 Variational Model

The mechanical response of granular materials can be computed from variational models defined within the context of Cosserat continuum theory. Let Ω be a bounded domain with Lipschitz boundary $\partial\Omega$ and $\mathbf{u} : \Omega \subset \mathbb{R}^d \mapsto \mathbb{R}^d$ be the displacement vector field where d being the dimension of the problem under consideration, $\boldsymbol{\Phi} : \Omega \subset \mathbb{R}^d \mapsto \mathfrak{so}(d) := \left\{ R \in \mathbb{M}^{d\times d} \mid R^T = -R \right\}$ be the microrotations such that the micromotions of the particles are collected in the vector field $\boldsymbol{\varphi} = axl(\boldsymbol{\Phi}) : \Omega \subset \mathbb{R}^d \mapsto \mathbb{R}^d$, then the deformed configuration of these materials can be completely determined from the following minimization problem

$$\inf_{\mathbf{u},\boldsymbol{\Phi},\boldsymbol{\varphi}} \left\{ I\left(\mathbf{u}, \boldsymbol{\Phi}, \boldsymbol{\varphi}\right) \,;\, (\mathbf{u}, \boldsymbol{\Phi}, \boldsymbol{\varphi}) \in W^{1,p}\left(\Omega, \mathbb{R}^d\right) \times W^{1,p}\big(\Omega, \mathfrak{so}\left(d\right)\big) \times W^{1,p}\left(\Omega, \mathbb{R}^d\right) \right\}, \tag{5}$$

along with the prescribed boundary conditions $\mathbf{u}|_{\partial\Omega_u} = \mathbf{u}_\circ$ and $\boldsymbol{\varphi}|_{\partial\Omega_\varphi} = \boldsymbol{\varphi}_\circ$. Here $W^{1,p}$ is the space of admissible deformations (also known as Sobolev space) with

$p \in (1, \infty)$ related to the growth of the energy function W. The integral functional I is defined as

$$I(\mathbf{u}, \boldsymbol{\Phi}, \boldsymbol{\varphi}) = \int_{\Omega} W(\nabla \mathbf{u}, \boldsymbol{\Phi}, \nabla \boldsymbol{\varphi}) \, dV - \ell(\mathbf{u}, \boldsymbol{\varphi}), \tag{6}$$

where the potential ℓ takes the contribution of external forces $\mathbf{b}$, external couples $\mathbf{m}$, traction forces $\mathbf{t}_u$ and traction moments $\mathbf{t}_\varphi$ such that

$$\ell(\mathbf{u}, \boldsymbol{\varphi}) = \int_{\Omega} (\mathbf{b} \cdot \mathbf{u} + \mathbf{m} \cdot \boldsymbol{\varphi}) \, dV + \int_{\partial \Omega_u} \mathbf{t}_u \cdot \mathbf{u} \, dS + \int_{\partial \Omega_\varphi} \mathbf{t}_\varphi \cdot \boldsymbol{\varphi} \, dS. \tag{7}$$

In reality, the deformation of granular media is a dissipative process which should not be discussed in terms of energies and displacements. In this sense, our model only covers the initiation of material microstructures. For a full description of extended time-intervals, the variables $\mathbf{u}, \boldsymbol{\Phi}, \boldsymbol{\varphi}$ would have to be replaced by their corresponding velocities and the energy W by a dissipation function. An exposition of this procedure in the case of rigid elasticity can be found in [61–63].

Within the framework of generalized elasticity the mechanical response of granular materials can be determined with the specification of an energy potential that depends, in an independent way, on the particle displacement and microrotations. It is therefore possible to replace the energy potential W in the integral functional (6) by the following Cosserat energy function

$$W^{csrt}(\nabla \mathbf{u}, \boldsymbol{\Phi}, \nabla \boldsymbol{\varphi}) = \frac{1}{2} \boldsymbol{e}(\mathbf{u}, \boldsymbol{\varphi}) : \mathbb{C} : \boldsymbol{e}(\mathbf{u}, \boldsymbol{\varphi}) + \frac{1}{2} \boldsymbol{\kappa}(\boldsymbol{\varphi}) : \overline{\mathbb{C}} : \boldsymbol{\kappa}(\boldsymbol{\varphi}), \tag{8}$$

which do not only depends on the gradients of the macro and micro-motions of the particles but also on a relative macro-rotational deformation tensor $\boldsymbol{\Phi}$ that associates the macro-deformation with the micro-deformation of the particles. Here, $\boldsymbol{e} = \nabla \mathbf{u} - \boldsymbol{\Phi}$ is the Cosserat deformation strain tensor, $\boldsymbol{\kappa} = \nabla \boldsymbol{\varphi}$ is the rotational deformation strain tensor, $\mathbb{C}$ and $\overline{\mathbb{C}}$ are the fourth order constitutive tensors of elastic constants.

The earlier discussion in Sect. 2 on the intergranular interactions and counter rotations of the particles leads us to introduce an enhanced energy potential for the granular materials. In this spirit, the interaction energy potential (4) is integrated with the Cosserat energy function (8) to model the microstructures of the granular materials. This enables us to define a new enhanced energy potential for the granular materials in a Cosserat medium which is given by

$$W(\nabla \mathbf{u}, \boldsymbol{\Phi}, \nabla \boldsymbol{\varphi}) = \underbrace{W^{csrt}(\nabla \mathbf{u}, \boldsymbol{\Phi}, \nabla \boldsymbol{\varphi})}_{\text{Cosserat energy function}} + \underbrace{\alpha \left(\|\nabla \boldsymbol{\varphi}\|^2 - \beta^2 \|\operatorname{dev} \operatorname{sym} \nabla \mathbf{u}\|^2 \right)^2}_{\text{Interaction energy potential}}. \tag{9}$$

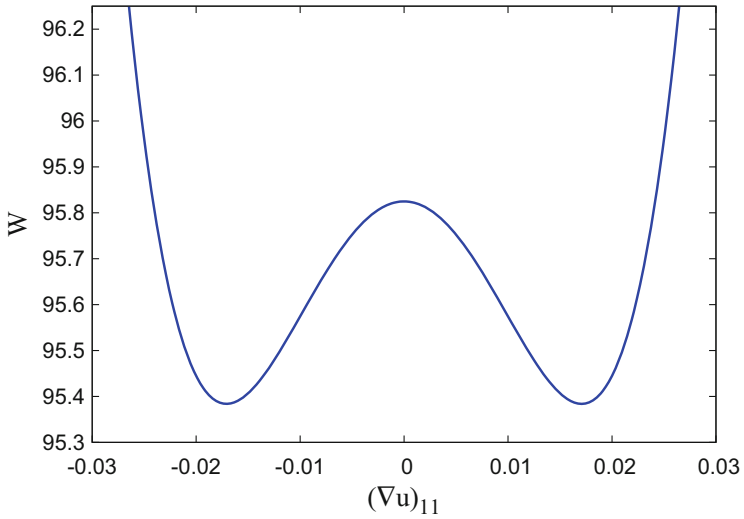

Fig. 2 Unrelaxed energy (10) curve for $E = 2.0 \times 10^2$ (MPa), $\nu = 0.3$, $\mu_c = 1.0 \times 10^{-2}$ (MPa), $\overline{\lambda} = 1.15 \times 10^2$ (N), $\overline{\mu} = 7.69 \times 10^1$ (N), $\overline{\mu}_c = 1.00 \times 10^1$ (N), $\alpha = 1.0 \times 10^1$ (N.mm^2) and $\beta = 1.20 \times 10^2$ (mm^{-1})

In an isotropic elastic Cosserat medium the enhanced energy potential (9) takes the form

$$W(\nabla \mathbf{u}, \boldsymbol{\Phi}, \nabla \boldsymbol{\varphi}) = \left(\frac{\lambda}{2} + \frac{\mu}{d}\right)(\operatorname{tr} \boldsymbol{\varepsilon})^2 + \mu \|\operatorname{dev} \boldsymbol{\varepsilon}\|^2 + \mu_c \|\operatorname{asy} \nabla \mathbf{u} - \boldsymbol{\Phi}\|^2 + \frac{\overline{\lambda}}{2}(\operatorname{tr} \boldsymbol{\kappa})^2 + \overline{\mu} \|\operatorname{sym} \boldsymbol{\kappa}\|^2 + \overline{\mu}_c \|\operatorname{asy} \boldsymbol{\kappa}\|^2 + \alpha \left(\|\operatorname{sym} \boldsymbol{\kappa}\|^2 + \|\operatorname{asy} \boldsymbol{\kappa}\|^2 - \beta^2 \|\operatorname{dev} \boldsymbol{\varepsilon}\|^2\right)^2 \tag{10}$$

Here, λ, μ, μ_c, $\bar{\lambda}$, $\bar{\mu}$, $\bar{\mu}_c$ are the Cosserat material constants.

The nonconvexity and hence the non-quasiconvexity of the energy potential (10) along some chosen strain paths can be seen from Fig. 2. Such non-quasiconvex energy potential when enters in (6) will lead to work with non-quasiconvex energy minimization problem whose general analytical solutions are always of interest. But, the solutions to such non-quasiconvex energy minimization problems do not exist in general, which is highly due to fine scale oscillations of the gradients of infimizing deformations. Here, in this case, the non-existence of these solutions is due to the possible displacement and microrotation field fluctuations at fine scales. The fine scale oscillations of the minimizing displacement and microrotation field variables will lead to the development of internal structures in the material. Formation of such microstructures can be extended microstructures [6, 33] which is distributed through the material domain or the localized microstructures [11, 27] which appear in the form of narrow shearing bands. Moreover, the existence of the unique minimizing translational and microrotational deformations are not guaranteed in this situation.

Thus to avoid these problems and to resolve the internal structures of the materials in consideration it is therefore necessary to compute a quasiconvex (relaxed) energy potential W^{rel}. The relaxed potential when enters in the minimization problem (5) now assures the ellipticity of the resulting boundary value problem, since it satisfy the Legendre-Hadamard condition (see definition by Ball and Dacorogna [7, 25]). The study by Morrey [41], Dacorogna [25, 26] gives sufficient justification for the relation of Legendre-Hadamard (ellipticity) condition with the constitutive description of a related mechanical problem.

If possible to compute the exact relaxed envelope of the corresponding non-quasiconvex energy in the energy minimization problem (5) one do not only guarantee general solutions of the associated energy minimization problem but also can predict on the formation of both the extended and localized microstructures in the materials. It is worth mentioning that, in this case, we are enable to compute an exact relaxed (quasi-convex) energy envelope corresponding to the non-quasiconvex energy potential in (10).

Since quasiconvex envelopes possess only degenerate ellipticity, only existence of minimizers can be guaranteed, no uniqueness. For numerical purposes it is therefore advantageous to add a very small strongly elliptic regularization term. This does not alter the character of the calculated solutions.

3.2 Computation of Relaxed Energy Envelope

In this section, we present our main result concerning the solutions of non-quasiconvex energy minimization problem in (5). In this respect, we compute an exact quasiconvex envelope of the energy function in (10). For other cases where it was possible to construct exact relaxed envelopes corresponding to energy minimization problems addressing different mechanical aspects the reader is referred to the work by Conti and Theil [24], Conti and Ortiz [23], Conti et al. [22], DeSimone and Dolzmann [28], Dret and Raoult [30], Kohn [36], Kohn and Strang [37, 38], Kohn and Vogelius [39], Raoult [50]. The quasiconvex envelope which here termed as the relaxed energy W^{rel} is thus stated as

Theorem 1 *Assume* $d = 3$, λ, μ, μ_c, $\bar{\lambda}$, $\bar{\mu}$, $\bar{\mu}_c$, α, $\beta \geq 0$, $\mu_\circ = \min\{\bar{\mu}, \bar{\mu}_c\}$. *Let*

$$f = \mu_\circ\, s + \mu\, c + \alpha \left(s - \beta^2\, c\right)^2, \qquad h = \begin{cases} (\bar{\mu} - \bar{\mu}_c)\ \|\text{sym}\ \boldsymbol{\kappa}\|^2 & \text{if } \bar{\mu} \geq \bar{\mu}_c \\ (\bar{\mu}_c - \bar{\mu})\ \|\text{asy}\ \boldsymbol{\kappa}\|^2 & \text{otherwise} \end{cases}$$

and define g *by*

$$g = \min_{\substack{s,c;\ c \geq \|\text{dev}\,\boldsymbol{\varepsilon}\|^2, \\ s \geq \left(\|\text{sym}\ \boldsymbol{\kappa}\|^2 + \|\text{asy}\ \boldsymbol{\kappa}\|^2\right)}} f(s, c)\,. \tag{11}$$

Then, the quasicovnex envelope of the Cosserat strain energy defined in (10) is given by

$$W^{rel} = \left(\frac{\lambda}{2} + \frac{\mu}{d}\right)\left(\operatorname{tr}\boldsymbol{\varepsilon}\right)^2 + \mu_c \left\|\operatorname{asy}\nabla\mathbf{u} - \boldsymbol{\Phi}\right\|^2 + \frac{\overline{\lambda}}{2}\left(\operatorname{tr}\boldsymbol{\kappa}\right)^2 + h + g\left(\left\|\operatorname{sym}\boldsymbol{\kappa}\right\|^2, \left\|\operatorname{asy}\boldsymbol{\kappa}\right\|^2, \left\|\operatorname{dev}\boldsymbol{\varepsilon}\right\|^2\right). \tag{12}$$

Proof Consider the rank-one line $\boldsymbol{\kappa}_t = \boldsymbol{\kappa} + t\,\mathbf{a}\otimes\mathbf{b}$; $\mathbf{a},\mathbf{b}\in\mathbb{R}^d$, $t\in\mathbb{R}$, then

$$W\left(\boldsymbol{e},\boldsymbol{\kappa}_t\right) = \left(\frac{\lambda}{2} + \frac{\mu}{d}\right)\left(\operatorname{tr}\boldsymbol{\varepsilon}\right)^2 + \mu\left\|\operatorname{dev}\boldsymbol{\varepsilon}\right\|^2 + \mu_c\left\|\operatorname{asy}\nabla\mathbf{u} - \boldsymbol{\Phi}\right\|^2 + \frac{\overline{\lambda}}{2}\left(\operatorname{tr}\boldsymbol{\kappa}\right)^2 + \overline{\mu}\left\|\operatorname{sym}\boldsymbol{\kappa}_t\right\|^2 + \overline{\mu}_c\left\|\operatorname{asy}\boldsymbol{\kappa}_t\right\|^2 + \alpha\left(\left\|\operatorname{sym}\boldsymbol{\kappa}_t\right\|^2 + \left\|\operatorname{asy}\boldsymbol{\kappa}_t\right\|^2 - \beta^2\left\|\operatorname{dev}\boldsymbol{\varepsilon}\right\|^2\right)^2 \tag{13}$$

Now, for any $s \geq \|\boldsymbol{\kappa}\|^2$ we can select $t_- < t \leq 0$ such that $\|\boldsymbol{\kappa}_t\|^2 = s$. A lamination in this direction gives

$$W^{rc} \leq \left(\frac{\lambda}{2} + \frac{\mu}{d}\right)\left(\operatorname{tr}\boldsymbol{\varepsilon}\right)^2 + \mu_c\left\|\operatorname{asy}\nabla\mathbf{u} - \boldsymbol{\Phi}\right\|^2 + \frac{\overline{\lambda}}{2}\left(\operatorname{tr}\boldsymbol{\kappa}\right)^2 + h + \min_{s\geq\|\operatorname{sym}\boldsymbol{\kappa}\|^2+\|\operatorname{asy}\boldsymbol{\kappa}\|^2}\left\{\mu_\circ\, s + \mu\left\|\operatorname{dev}\boldsymbol{\varepsilon}\right\|^2 + \alpha\left(s - \beta^2\left\|\operatorname{dev}\boldsymbol{\varepsilon}\right\|^2\right)^2\right\}. \tag{14}$$

Here, rc in the superscript stands for rank-one convex envelope. Working along the rank-one line $\boldsymbol{e}_t = \boldsymbol{e} + t\,\mathbf{c}\otimes\mathbf{d}$; $\mathbf{c},\mathbf{d}\in\mathbb{R}^d$ and following the arguments above, we obtain

$$W^{rc} \leq \left(\frac{\lambda}{2} + \frac{\mu}{d}\right)\left(\operatorname{tr}\boldsymbol{\varepsilon}\right)^2 + \mu_c\left\|\operatorname{asy}\nabla\mathbf{u} - \boldsymbol{\Phi}\right\|^2 + \frac{\overline{\lambda}}{2}\left(\operatorname{tr}\boldsymbol{\kappa}\right)^2 + h + \min_{c\geq\|\operatorname{dev}\boldsymbol{\varepsilon}\|^2}\left\{\mu_\circ\left(\left\|\operatorname{sym}\boldsymbol{\kappa}\right\|^2 + \left\|\operatorname{asy}\boldsymbol{\kappa}\right\|^2\right) + \mu\, c + \alpha\left(\left\|\operatorname{sym}\boldsymbol{\kappa}\right\|^2 + \left\|\operatorname{asy}\boldsymbol{\kappa}\right\|^2 - \beta^2 c\right)^2\right\}. \tag{15}$$

Hence the upper bound is proved. The lower bound is based on Lemma 1 below and on the fact that, for $h_1 : [0,\infty)^d \mapsto \mathbb{R}^d$ convex and non-decreasing in each variable and $h_2 : \mathbb{R}^{d\times d} \mapsto \mathbb{R}^d$ component-wise convex, the function $h_1 \circ h_2$ is convex. This completes the proof.

Lemma 1 *Let $f : [0, \infty)^2 \mapsto [0, \infty)$ be convex. Then the function g defined by*

$$g(x) = \inf_{s_1 \geq x_1, s_2 \geq x_2} f(s) \tag{16}$$

is convex and non-decreasing in each variable.

Proof Fix $x', x'', \lambda \in (0, 1)$. For any $\epsilon > 0$ there are s', s'' such that $x' \leq s', x'' \leq s''$, and

$$f(s') \leq g(x') + \epsilon, \quad f(s'') \leq g(x'') + \epsilon. \tag{17}$$

Then $\lambda s' + (1 - \lambda)s'' \geq \lambda x' + (1 - \lambda)x''$, and since f is convex we obtain

$$\begin{aligned} g(\lambda x' + (1 - \lambda)x'') &\leq f(\lambda s' + (1 - \lambda)s'') \leq \lambda f(s') + (1 - \lambda) f(s'') \\ &\leq \lambda g(x') + (1 - \lambda) g(x'') + \epsilon. \end{aligned} \tag{18}$$

Therefore g is convex. Monotonicity is clear from the definition.

To compute the exact relaxed envelope in (12) one needs to solve the minimization problem (11). The stationarity conditions to this minimization problem are as follows

3.2.1 Stationarity Conditions

$$\text{(1). for } \quad s = \|\operatorname{sym} \boldsymbol{\kappa}\|^2 + \|\operatorname{asy} \boldsymbol{\kappa}\|^2 \text{ and } \quad c \geq \|\operatorname{dev} \boldsymbol{\varepsilon}\|^2 : \quad \frac{\partial g}{\partial c} = 0, \quad \frac{\partial g}{\partial s} \geq 0, \tag{19a}$$

$$\text{(2). for } \quad s = \|\operatorname{sym} \boldsymbol{\kappa}\|^2 + \|\operatorname{asy} \boldsymbol{\kappa}\|^2 \text{ and } \quad c = \|\operatorname{dev} \boldsymbol{\varepsilon}\|^2 : \quad \frac{\partial g}{\partial c} \geq 0, \quad \frac{\partial g}{\partial s} \geq 0, \tag{19b}$$

$$\text{(3). for } \quad c = \|\operatorname{dev} \boldsymbol{\varepsilon}\|^2 \text{ and } \quad s \geq \|\operatorname{sym} \boldsymbol{\kappa}\|^2 + \|\operatorname{asy} \boldsymbol{\kappa}\|^2 : \quad \frac{\partial g}{\partial s} = 0, \quad \frac{\partial g}{\partial c} \geq 0. \tag{19c}$$

On the basis of these three stationarity conditions the material energy can be characterized into the following three phases

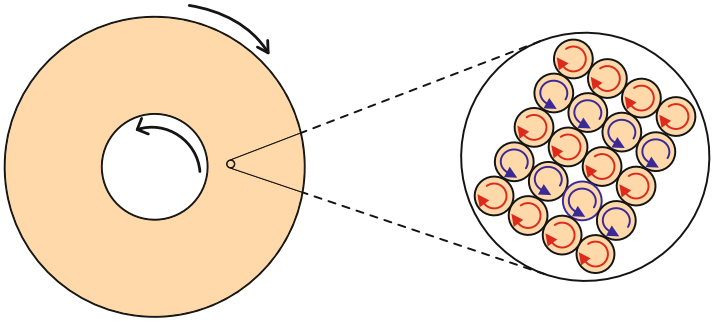

Fig. 3 A Couette shear cell where the two arrows indicates the shearing direction of the inner and outer boundaries of the annular domain. In inset the microstructure patterns due to microrotational motions of the particles is shown

3.2.2 Material Phase with Microstructure in Microrotational Motions (Micromotions) (Phase 1)

This phase is corresponding to the material regime where there are microstructures due to the micromotions (which are in fact the rotational degrees of freedom assembled in the microrotational vector field $\boldsymbol{\varphi}$) of the continuum particles. A schematic representation of such microstructure is given in Fig. 3. The enhanced energy potential (10) is nonconvex in this microstructural phase. It is observed that whenever the norm of the curvature strain tensor is dominating over the norm of the macroscopic shear strain tensor for some specific choice of the material parameters μ, α and β, the material experiences a microstructure in micromotions. This microstructural material phase is characterized by the following inequality relation

$$\|\boldsymbol{\kappa}\|^2 \geq \beta^2 \|\operatorname{dev} \boldsymbol{\varepsilon}\|^2 + \frac{\mu}{2\alpha\beta^2}. \tag{20}$$

It is important to note the effect of shear modulus μ, internal length scale (e.g., the diameter of particles) β and the coherency interaction modulus or frictional modulus α in conjunction with the curvature and macroscopic shear strains which plays very crucial role in the observation of this internal structural phase of the material. Using the first stationarity condition (19a) the minimizers of the problem in (11) are obtained as

$$s = \|\operatorname{sym} \boldsymbol{\kappa}\|^2 + \|\operatorname{asy} \boldsymbol{\kappa}\|^2, \qquad c = \frac{1}{\beta^2}\left(\|\operatorname{sym} \boldsymbol{\kappa}\|^2 + \|\operatorname{asy} \boldsymbol{\kappa}\|^2\right) - \frac{\mu}{2\alpha\beta^4}. \tag{21}$$

Thus, the scalar convex function g is given by

$$g = \begin{cases} \left(\overline{\mu} - \overline{\mu}_c + \mu_\circ + \frac{\mu}{\beta^2}\right) \|\text{sym } \boldsymbol{\kappa}\|^2 + \left(\mu_\circ + \frac{\mu}{\beta^2}\right) \|\text{asy } \boldsymbol{\kappa}\|^2 - \frac{\mu^2}{4\alpha\beta^4} & \text{if} \quad \bar{\mu} \geq \bar{\mu}_c \\ \left(\mu_\circ + \frac{\mu}{\beta^2}\right) \|\text{sym } \boldsymbol{\kappa}\|^2 + \left(\overline{\mu}_c - \overline{\mu} + \mu_\circ + \frac{\mu}{\beta^2}\right) \|\text{asy } \boldsymbol{\kappa}\|^2 - \frac{\mu^2}{4\alpha\beta^4} & \text{if} \quad \bar{\mu} < \bar{\mu}_c \end{cases} \tag{22}$$

The relaxed energy of the material in this phase is obtained as

$$W_1^{rel} = \begin{cases} \left(\frac{\lambda}{2} + \frac{\mu}{d}\right) \left(\text{tr } \boldsymbol{\varepsilon}\right)^2 + \mu_c \|\text{asy } \nabla \mathbf{u} - \mathscr{E} \cdot \boldsymbol{\varphi}\|^2 - \frac{\mu^2}{4\alpha\beta^4} \\ + \frac{\bar{\lambda}}{2} (\text{tr } \boldsymbol{\kappa})^2 + (\bar{\mu} - \bar{\mu}_c) \|\text{sym } \boldsymbol{\kappa}\|^2 + \left(\mu_\circ + \frac{\mu}{\beta^2}\right) \|\boldsymbol{\kappa}\|^2 \end{cases} \quad \text{if} \quad \bar{\mu} \geq \bar{\mu}_c,$$

$$\begin{cases} \left(\frac{\lambda}{2} + \frac{\mu}{d}\right) \left(\text{tr } \boldsymbol{\varepsilon}\right)^2 + \mu_c \|\text{asy } \nabla \mathbf{u} - \mathscr{E} \cdot \boldsymbol{\varphi}\|^2 - \frac{\mu^2}{4\alpha\beta^4} \\ + \frac{\bar{\lambda}}{2} (\text{tr } \boldsymbol{\kappa})^2 - (\bar{\mu} - \bar{\mu}_c) \|\text{asy } \boldsymbol{\kappa}\|^2 + \left(\mu_\circ + \frac{\mu}{\beta^2}\right) \|\boldsymbol{\kappa}\|^2 \end{cases} \quad \text{if} \quad \bar{\mu} < \bar{\mu}_c \tag{23}$$

3.2.3 Material Phase with No Microstructure (Phase 2)

This phase is connected with the material regime where there is no internal structure in the material. The second stationarity condition (19b) clearly shows that the minimizers of the functional in (11) are itself $\left(\|\text{sym } \boldsymbol{\kappa}\|^2 + \|\text{asy } \boldsymbol{\kappa}\|^2\right)$ and $\|\text{dev } \boldsymbol{\varepsilon}\|^2$ respectively. This indicates that the original energy potential in (10) is convex in this material phase. The criteria for the recognition of this material phase is given by the following inequality relation

$$\beta^2 \|\text{dev } \boldsymbol{\varepsilon}\|^2 - \frac{\mu_\circ}{2\alpha} \leq \|\boldsymbol{\kappa}\|^2 \leq \beta^2 \|\text{dev } \boldsymbol{\varepsilon}\|^2 + \frac{\mu}{2\alpha\beta^2}. \tag{24}$$

The function g in this phase is given by

$$\begin{aligned} g \;=\; & \overline{\mu} \|\text{sym } \boldsymbol{\kappa}\|^2 \;+\; \overline{\mu}_c \|\text{asy } \boldsymbol{\kappa}\|^2 \;+\; \mu \|\text{dev } \boldsymbol{\varepsilon}\|^2 \\ & + \alpha \left(\|\text{sym } \boldsymbol{\kappa}\|^2 \;+\; \|\text{asy } \boldsymbol{\kappa}\|^2 \;-\; \beta^2 \|\text{dev } \boldsymbol{\varepsilon}\|^2\right)^2. \end{aligned} \tag{25}$$

The relaxed energy potential in this phase is thus the original energy potential (10) itself and we write

$$W_2^{rel} = \left(\frac{\lambda}{2} + \frac{\mu}{d}\right)\left(\operatorname{tr}\boldsymbol{\varepsilon}\right)^2 + \mu\,\|\operatorname{dev}\boldsymbol{\varepsilon}\|^2 + \mu_c\,\|\operatorname{asy}\nabla\mathbf{u} - \mathscr{E}\cdot\boldsymbol{\varphi}\|^2 + \frac{\overline{\lambda}}{2}\left(\operatorname{tr}\boldsymbol{\kappa}\right)^2 + \overline{\mu}\,\|\operatorname{sym}\boldsymbol{\kappa}\|^2 + \overline{\mu}_c\,\|\operatorname{asy}\boldsymbol{\kappa}\|^2 + \alpha\left(\|\operatorname{sym}\boldsymbol{\kappa}\|^2 + \|\operatorname{asy}\boldsymbol{\kappa}\|^2 - \beta^2\,\|\operatorname{dev}\boldsymbol{\varepsilon}\|^2\right)^2 \tag{26}$$

3.2.4 Material Phase with Microstructure in Translational Motions (Phase 3)

This phase constitutes an unexpected outcome of the theory presented. It consists of laminates formed by alternating displacements as for example formed by phase-transforming materials. It would be interesting to see whether such structures can be observed experimentally.

This phase is related to the material regime where there is a microstructure in translational motions (which are in fact the displacement degrees of freedom of the continuum particles and are assembled in the displacement vector field $\mathbf{u}$) of the continuum particles. A schematic representation of such microstructure formation is shown in Fig. 4. The enhanced energy potential (10) thus becomes nonconvex in this phase. Using the third stationarity condition (19c) it is observed that the norm of the macroscopic shear strain tensor is dominating over the norm of the rotational strain tensor. The material is said to be in this phase whenever the following criteria is satisfied

$$\beta^2\,\|\operatorname{dev}\boldsymbol{\varepsilon}\|^2 - \frac{\mu_\circ}{2\alpha} \geq \|\boldsymbol{\kappa}\|^2\,. \tag{27}$$

It is important to note the effect the coherency modulus α and the Cosserat material modulus $\mu_\circ$ in the characterization of this microstructural phase. The minimizers of the functional in (11) are obtained after solving the third stationarity condition (19c)

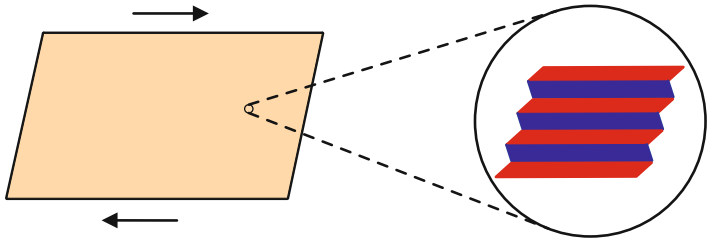

Fig. 4 A rectangular specimen under shear with two arrow head pointing towards the shearing direction. In inset the microstructure patterns formed due to the translational motions of the continuum particles is shown

which are given as

$$c \;=\; \|\mathrm{dev}\,\boldsymbol{\varepsilon}\|^2 \qquad \text{and} \qquad s \;=\; \beta^2\;\|\mathrm{dev}\,\boldsymbol{\varepsilon}\|^2 - \frac{\mu_\circ}{2\alpha}. \tag{28}$$

Thus minimum potential g in (11) takes the following form

$$g \;=\; \begin{cases} \left(\overline{\mu} - \overline{\mu}_c\right)\|\mathrm{sym}\;\boldsymbol{\kappa}\|^2 + \left(\mu_\circ\beta^2 + \mu\right)\;\|\mathrm{dev}\,\boldsymbol{\varepsilon}\|^2 - \dfrac{\mu_\circ^2}{4\alpha} & \text{if} \quad \bar{\mu} \geq \bar{\mu}_c \\[2ex] \left(\overline{\mu}_c - \overline{\mu}\right)\|\mathrm{asy}\;\boldsymbol{\kappa}\|^2 + \left(\mu_\circ\beta^2 + \mu\right)\;\|\mathrm{dev}\,\boldsymbol{\varepsilon}\|^2 - \dfrac{\mu_\circ^2}{4\alpha} & \text{if} \quad \bar{\mu} < \bar{\mu}_c \end{cases} \tag{29}$$

Hence the relaxed energy potential in this phase is obtained as

$$W_3^{rel} \;=\; \begin{cases} \left(\dfrac{\lambda}{2} + \dfrac{\mu}{d}\right)\left(\mathrm{tr}\;\boldsymbol{\varepsilon}\right)^2 + \mu_c\,\|\mathrm{asy}\;\nabla\mathbf{u} - \mathscr{E}\cdot\boldsymbol{\varphi}\|^2 + \dfrac{\bar{\lambda}}{2}(\mathrm{tr}\;\boldsymbol{\kappa})^2 & \\[2ex] \quad +(\bar{\mu} - \bar{\mu}_c)\,\|\mathrm{sym}\;\boldsymbol{\kappa}\|^2 + \left(\mu_\circ\beta^2 + \mu\right)\|\mathrm{dev}\,\boldsymbol{\varepsilon}\|^2 - \dfrac{{\mu_\circ}^2}{4\alpha} & \text{if} \quad \bar{\mu} \geq \bar{\mu}_c \\[2ex] \left(\dfrac{\lambda}{2} + \dfrac{\mu}{d}\right)\left(\mathrm{tr}\;\boldsymbol{\varepsilon}\right)^2 + \mu_c\,\|\mathrm{asy}\;\nabla\mathbf{u} - \mathscr{E}\cdot\boldsymbol{\varphi}\|^2 + \dfrac{\bar{\lambda}}{2}\,(\mathrm{tr}\;\boldsymbol{\kappa})^2 & \\[2ex] \quad -(\bar{\mu} - \bar{\mu}_c)\,\|\mathrm{asy}\;\boldsymbol{\kappa}\|^2 + \left(\mu_\circ\beta^2 + \mu\right)\|\mathrm{dev}\,\boldsymbol{\varepsilon}\|^2 - \dfrac{{\mu_\circ}^2}{4\alpha} & \text{if} \quad \bar{\mu} < \bar{\mu}_c \end{cases} \tag{30}$$

3.2.5 Relaxed Energy

The total relaxed energy thus comprises all the three energies in each of the phase and it acquires finally the following form

$$W^{rel} \;=\; \begin{cases} W_1^{rel} & \text{if} \quad \|\boldsymbol{\kappa}\|^2 \geq \beta^2\,\|\mathrm{dev}\,\boldsymbol{\varepsilon}\|^2 + \dfrac{\mu}{2\alpha\beta^2} \\[2ex] W_2^{rel} & \text{if} \quad -\dfrac{\mu_\circ}{2\alpha} \leq \|\boldsymbol{\kappa}\|^2 - \beta^2\,\|\mathrm{dev}\,\boldsymbol{\varepsilon}\|^2 \leq \dfrac{\mu}{2\alpha\beta^2} \\[2ex] W_3^{rel} & \text{if} \quad \|\boldsymbol{\kappa}\|^2 \leq \beta^2\,\|\mathrm{dev}\,\boldsymbol{\varepsilon}\|^2 - \dfrac{\mu_\circ}{2\alpha} \end{cases} \tag{31}$$

where W_1^{rel}, W_2^{rel} and W_3^{rel} are explicitly given as in (23), (26) and (30), respectively. The computation of this analytical expression for the relaxed energy corresponding to non-quasiconvex energy function in (10) thus enable us to

predict all microstructural features of the material which are carried safely from the microscopic to macroscopic computational scale. Hence we have extracted all possible information regarding the development of microstructural regimes in the granular materials pertinent to observing its macro-mechanical behavior. For practical applications it is now more efficient and effective to reformulate the original non-quasiconvex problem in (5) to a relaxed energy minimization problem using this relaxed potential.

3.2.6 Nonlinear Constitutive Relations

The proposed granular material model is completed with the formulation of constitutive relations between stress and strain tensors in a Cosserat medium. The constitutive structure of the proposed theory thus comprises of three phases (as discussed in Sect. 3.2) where in each phase the force-stress are explicitly related to the Cosserat strain tensors according to the following formulas:

$$\boldsymbol{\sigma} = \begin{cases} 2\left(\frac{\lambda}{2}+\frac{\mu}{d}\right)\left(\operatorname{tr}\boldsymbol{\varepsilon}\right)\mathbf{I}+2\,\mu_c\left(\operatorname{asy}\nabla\mathbf{u}-\boldsymbol{\Phi}\right), & \text{(Phase 1)} \\ \begin{cases}\lambda\left(\operatorname{tr}\boldsymbol{\varepsilon}\right)\mathbf{I}+2\,\mu\,\boldsymbol{\varepsilon}+2\,\mu_c\left(\operatorname{asy}\nabla\mathbf{u}-\boldsymbol{\Phi}\right)\\ -4\,\alpha\,\beta^2\left(\|\boldsymbol{\kappa}\|^2-\beta^2\|\operatorname{dev}\boldsymbol{\varepsilon}\|^2\right)\left(\operatorname{dev}\boldsymbol{\varepsilon}\right),\end{cases} & \text{(Phase 2)} \\ \lambda\left(\operatorname{tr}\boldsymbol{\varepsilon}\right)\mathbf{I}+2\,\mu\,\boldsymbol{\varepsilon}+2\,\mu_\circ\beta^2\left(\operatorname{dev}\boldsymbol{\varepsilon}\right)+2\,\mu_c\left(\operatorname{asy}\nabla\mathbf{u}-\boldsymbol{\Phi}\right). & \text{(Phase 3)} \end{cases} \tag{32}$$

The couple-stress tensor is related to the curvature strain tensors by the following formulas:

$$\boldsymbol{\mu} = \begin{cases} \begin{cases}\bar{\lambda}\left(\operatorname{tr}\boldsymbol{\kappa}\right)\mathbf{I}+2\left(\bar{\mu}-\bar{\mu}_c\right)\left(\operatorname{sym}\boldsymbol{\kappa}\right)+2\left(\mu_\circ+\frac{\mu}{\beta^2}\right)\boldsymbol{\kappa} & \text{if}\quad \bar{\mu}\geq\bar{\mu}_c,\\ \bar{\lambda}\left(\operatorname{tr}\boldsymbol{\kappa}\right)\mathbf{I}-2\left(\bar{\mu}-\bar{\mu}_c\right)\left(\operatorname{asy}\boldsymbol{\kappa}\right)+2\left(\mu_\circ+\frac{\mu}{\beta^2}\right)\boldsymbol{\kappa} & \text{if}\quad \bar{\mu}<\bar{\mu}_c.\end{cases} & \text{(Phase 1)} \\ \begin{cases}\bar{\lambda}\left(\operatorname{tr}\boldsymbol{\kappa}\right)\mathbf{I}+2\,\bar{\mu}\left(\operatorname{sym}\boldsymbol{\kappa}\right)+2\,\bar{\mu_c}\left(\operatorname{asy}\boldsymbol{\kappa}\right)\\ +4\,\alpha\left(\|\operatorname{sym}\boldsymbol{\kappa}\|^2+\|\operatorname{asy}\boldsymbol{\kappa}\|^2-\beta^2\|\operatorname{dev}\boldsymbol{\varepsilon}\|^2\right)\boldsymbol{\kappa}\end{cases} & \text{(Phase 2)} \\ \begin{cases}\bar{\lambda}\left(\operatorname{tr}\boldsymbol{\kappa}\right)\mathbf{I}+2\left(\bar{\mu}-\bar{\mu}_c\right)\left(\operatorname{sym}\boldsymbol{\kappa}\right) & \text{if}\quad \bar{\mu}\geq\bar{\mu}_c,\\ \bar{\lambda}\left(\operatorname{tr}\boldsymbol{\kappa}\right)\mathbf{I}-2\left(\bar{\mu}-\bar{\mu}_c\right)\left(\operatorname{asy}\boldsymbol{\kappa}\right) & \text{if}\quad \bar{\mu}<\bar{\mu}_c.\end{cases} & \text{(Phase 3)} \end{cases} \tag{33}$$

4 Numerical Results

Based on one-dimensional numerical computations the mechanical response of the material is analyzed along some chosen macroscopic strain paths. A simple shear and a tension-compression tests are briefly presented to observe the development of microstructures which is characterized by the activation of different material regimes as discussed in the Sect. 3.2.

4.1 A Simple Shear Test

Consider a two dimensional domain $\Omega = (0, X_1) \times (0, X_2)$ where $(X_1, X_2) \in \mathbb{R}^2$. We choose the macroscopic strain paths as follows

$$\begin{aligned} \boldsymbol{\varepsilon} &= \frac{\gamma}{2} \left(\mathbf{e}_1 \otimes \mathbf{e}_2 + \mathbf{e}_2 \otimes \mathbf{e}_1 \right), \\ \boldsymbol{e} &= \gamma \, \mathbf{e}_2 \otimes \mathbf{e}_1 + \varphi_3 \left(\mathbf{e}_2 \otimes \mathbf{e}_1 - \mathbf{e}_1 \otimes \mathbf{e}_2 \right), \\ \boldsymbol{\omega}_e &= \left(\frac{\gamma}{2} + \varphi_3 \right) \left(\mathbf{e}_2 \otimes \mathbf{e}_1 - \mathbf{e}_1 \otimes \mathbf{e}_2 \right), \\ \boldsymbol{\kappa} &= b \left(\mathbf{e}_1 \otimes \mathbf{e}_3 + \mathbf{e}_2 \otimes \mathbf{e}_3 \right). \end{aligned} \tag{34}$$

Here, γ is the macroscopic shear, φ_3 is the material microrotational degree of freedom and b is some fixed curvature. We assume that φ_3 linearly depends on both of the material coordinates X_1 and X_2 such that $\varphi_3 = b(X_1 + X_2)$. In this analysis we take $b = \dfrac{\pi}{6}$ and calculate φ_3 for all those material points which lies on the line $X_1 + X_2 = 1$. Other than Lame's constants $\lambda = \dfrac{\nu \mathrm{E}}{(1+\nu)(1-2\nu)}$ and $\mu = \dfrac{\mathrm{E}}{2(1+\nu)}$ there are eight additional material parameters that are pertinent to the material microstructures and are described in Table 1. Initially the material experiences a microstructure in micromotions of the particles. Upon further loading it transforms its structure and enter into a regime where there is no microstructure in the material. Further, upon increasing the load it changes its state to a material regime where it experiences a microstructure in translational motions of the particles. It is observed that all three phases of the material structure with two microstructural regimes and one non-microstructural regime coexists. In Fig. 5a the constitutive response of the material is shown, where it is observed that the non-monotone stress-strain curve is replaced by its energetically equivalent Maxwell line corresponding to a uniform vanishing stress. This vanishing stress regime is corresponding to the regime of the material where it experiences a microstructure in micromotions of the particles. In the material regime where there is no internal structure a nonlinear constitutive response is seen. Whereas, in the material regime where there is a microstructure in translational motions of the particles we observe a linear constitutive response in this

Table 1 Material parameters for the analytical computations in a simple shear test

Parameter	Numerical value	Units	Parameter	Numerical value	Units
E	2.0×10^2	(MPa)	$\overline{\lambda}$	λ	(N)
μ_c	1.0×10^{-1}	(MPa)	$\overline{\mu}$	μ	(N)
ν	0.3	(—)	$\overline{\mu}_c$	μ_c	(N)
α	5.0×10^{-1}	(N.mm^2)	β	1.0×10^1	(mm^{-1})

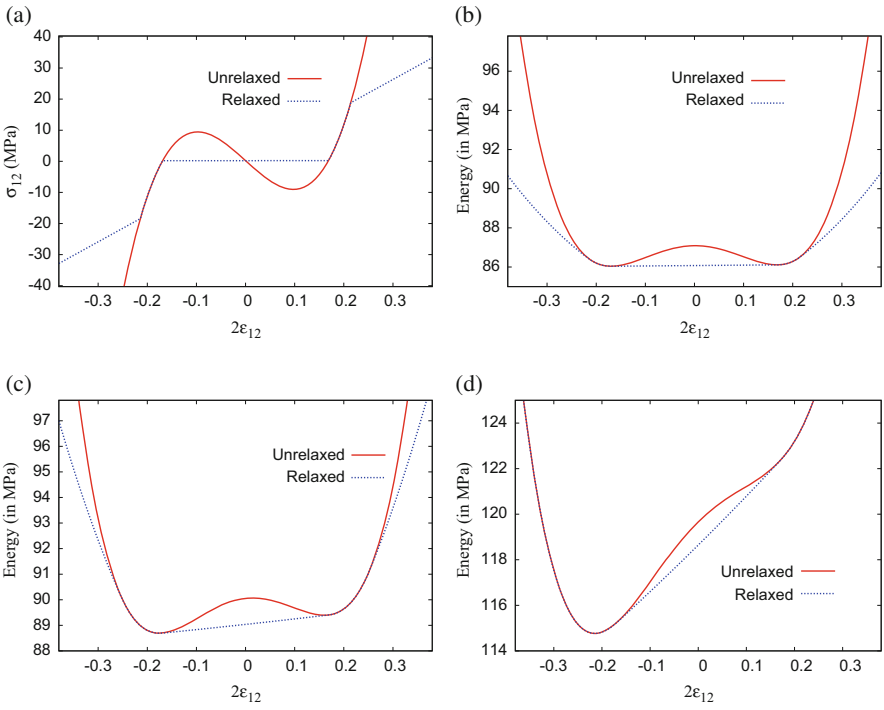

Fig. 5 (**a**) Relaxed and unrelaxed stress-strain curve in different material regimes; (**b**) Relaxed and unrelaxed curve for the Cosserat coupled modulus $\mu_c = 0.1$; (**c**) Relaxed and unrelaxed curve for the Cosserat coupled modulus $\mu_c = 1.0$; and, (**d**) Relaxed and unrelaxed curve for the Cosserat coupled modulus $\mu_c = 10.0$

one dimensional analysis. The corresponding nonconvex and relaxed energy plots are shown in Fig. 5b. In Fig. 5c and d the relaxed and unrelaxed energy is plotted for two different values of the Cosserat coupled modulus $\mu_c = 1.0$ and $\mu_c = 10.0$ respectively. These figures demonstrate that not only the particle size in granular material effects the development of microstructures but also the Cosserat coupled shear modulus do have influence in the development of material microstructures in granular materials.

Table 2 Material parameters for the analytical computations in a tension-compression test

Parameter	Numerical value	Units	Parameter	Numerical value	Units
E	2.0×10^2	(MPa)	$\overline{\lambda}$	1.15×10^2	(N)
μ_c	1.0×10^{-2}	(MPa)	$\overline{\mu}$	7.69×10^1	(N)
ν	0.3	(—)	$\overline{\mu}_c$	1.00×10^1	(N)
α	1.0×10^{-1}	(N.mm^2)	β	1.20×10^2	(mm^{-1})

4.2 A Tension-Compression Test

In this example the material behavior in a plain strain tension-compression test is investigated. The macroscopic strain tensors for this analysis takes the following form

$$\begin{aligned} \boldsymbol{\varepsilon} &= \delta\, \mathbf{e}_1 \otimes \mathbf{e}_1, \\ \boldsymbol{e} &= \delta\, \mathbf{e}_1 \otimes \mathbf{e}_1 + \varphi_3\, (\mathbf{e}_2 \otimes \mathbf{e}_1 - \mathbf{e}_1 \otimes \mathbf{e}_2)\,, \\ \boldsymbol{\omega}_e &= \varphi_3\, (\mathbf{e}_2 \otimes \mathbf{e}_1 - \mathbf{e}_1 \otimes \mathbf{e}_2)\,. \end{aligned} \tag{35}$$

Here δ is the macroscopic stretch. The Cosserat rotational strain tensor $\boldsymbol{\kappa}$ is taken to be the same as mentioned in the previous test. Moreover, the micro-rotational degree of freedom, φ_3 at each material point is calculated according to similar assumption as in the case of simple shear test. The material parameters are chosen as described in Table 2.

It is observed that all the three phases of material structure coexists in this case. The constitutive behavior in the material microstructural and non-microstructural regimes is shown in Fig. 6a where contrary to the case of shear test it is observed that the stress do not vanish in the regime where material experiences a microstructure in micromotions. Here the non-monotone stress-strain curve is replaced by its energetically equivalent monotone curve. This is due to the non-constant slope of the relaxed energy envelope in the globally non-convex range of the unrelaxed energy potential, as seen in magnified picture in Fig. 6b. Moreover, the properties of unrelaxed and relaxed energy envelope are studied for different values of the interaction modulus α and the material parameter β related to the particle size. A two-well energy structure is seen in Figure for three different values of the interaction modulus. Both the wells have same local minima. In Fig. 6c it is observed that by varying the interaction modulus the local minima of the energy envelope do not change. This is because the globally nonconvex range of these energy curves do not vary. However it is important to note that the locally non-convex range of these unrelaxed energy curves decreases with the increase in the interaction modulus. The computed relaxed energy is plotted in Fig. 6d where it is seen that by varying the interaction modulus the global minima of all the three energy curves do not change. The influence of the particle size on the material strain energy is observed in Figs. 6e and f. It is seen that the particle size do not only influence the range of local non-convexity of the energy potential but also its global non-convexity range.

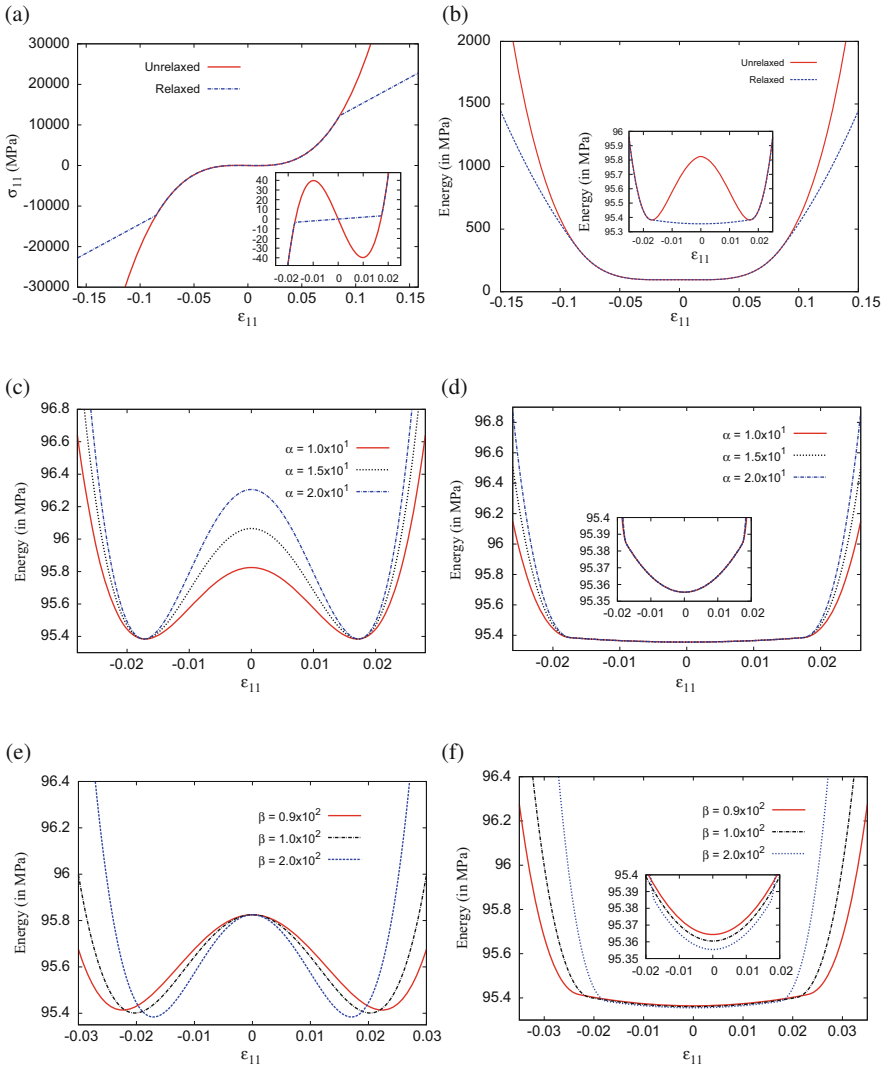

Fig. 6 (**a**) Relaxed and unrelaxed stress-strain curve in different regimes of the material; (**b**) Relaxed and unrelaxed energy curve in different material regimes; (**c**) Unrelaxed energy curves for varying values of the material parameter α; (**d**) Relaxed energy curves for varying values of the material parameter α; (**e**) Unrelaxed energy curves for varying values of the material parameter β; and, (**f**) Relaxed energy curves for varying values of the material parameter β

It is important to note that the local maxima of the energy potential do not change with the varying particle size. This is contrary to the case seen in Fig. 6c. Moreover, the local and global minima of the potential are shifted and get a lower values with the increased value of the material parameter β as seen in Figs. 6e and f.

5 Conclusion

In nature granular materials exhibit distinct patterns under deformation. The formation of these patterns is strongly influenced by counter-rotations of the interacting particle at the microscale. In this article, we study the counter-rotations of the particles and the formation of rotational microstructures in granular materials.

By employing the direct methods in the calculus of variations it turns out to be possible to derive an exact quasiconvex envelope of the energy potential. It is worth mentioning that there are no further assumptions necessary to derive this quasiconvex envelope. The computed relaxed potential yields all the possible displacement and micro-rotation field fluctuations as minimizers. Hence, by doing so we do not only resolve the issues concerning related non-quasiconvex variational problem but also guarantee the existence and uniqueness of energy minimizers. Moreover, the independence of these minimizers on the discretization of the spatial domain is ensured. We conclude with the result that the granular material behavior can be divided into three different regimes. Two of the material regimes are exhibiting microstructures in rotational and translational motions of the particles, respectively, and the third one is corresponding to the case where there is no internal structure of the deformation field.

The proposed model is analyzed numerically in one-dimensional case where the numerical computations performed are based on some chosen strain paths. We demonstrate on different properties of the computed relaxed potential in a simple shear and a tension-compression test. Moreover, It has been shown that all the material phases can co-exist.

Acknowledgements The first author gratefully acknowledge the funding by Higher Education Commission (HEC) of Pakistan and highly appreciate the support by Deutscher Akademischer Austausch Dienst (DAAD) for this research work.

References

1. Alonso-Marroquín, F., Vardoulakis, I., Herrmann, H.J., Weatherley, D., Mora, P.: Effect of rolling on dissipation in fault gouges. Phys. Rev. E **74**, 301–306 (2006). http://dx.doi.org/doi:10.1103/PhysRevE.74.031306
2. Alsaleh, M.I., Voyiadjis, G.Z., Alshibli, K.A.: Modeling strain localization in granular materials using micropolar theory: Mathematical formulations. Int. J. Numer. Anal. Meth. Goemech. **30**, 1501–1524 (2006). http://dx.doi.org/doi:10.1002/nag.533
3. Alshibli, K.A., Alsaleh, M.I., Voyiadjis, G.Z.: Modelling strain localization in granular materials using micropolar theory: Numerical implementation and verification. Int. J. Numer. Anal. Meth. Goemech. **30**, 1525–1544 (2006). http://dx.doi.org/doi:10.1002/nag.534
4. Aranda, E., Pedregal, P.: Numerical approximation of non-homogeneous, non-convex vector variational problems. Numer. Math. **89**, 425–444 (2001). http://dx.doi.org/doi:10.1007/s002110100294
5. Aranson, I., Tsimring, L.: Granular Patterns. Oxford University Press, Oxford (2009)

6. Bagnold, R.A.: The Physics of Blown Sand and Desert Dunes. Methuen and Co. Ltd., London (1941)
7. Ball, J.M.: Convexity conditions and existence theorems in nonlinear elasticity. Arch. Ration. Mech. Anal. **63**, 337–403 (1976). http://dx.doi.org/doi:10.1007/BF00279992
8. Ball, J.M., James, R.D.: Fine phase mixtures as minimizers of energy. Arch. Ration. Mech. Anal. **100**, 13–52 (1987). http://dx.doi.org/doi:10.1007/bf00281246
9. Bardet, J.P.: Observation on the effects of particle rotations on the failure of idealized granular materials. Mech. Mater. **8**, 159–182 (1994). http://dx.doi.org/doi:10.1016/0167-6636(94)00006-9
10. Bartels, S.: Numerical Analysis of Some Non-Convex Variational Problems. PhD thesis. Christian-Alberechts-Universität, Kiel (2001)
11. Bauer, E., Huang, W.: Numerical investigation of strain localization in a hypoplastic cosserat material under shearing. In: Desai (ed.) Proceedings of the 10th International Conference on Computer Methods and Advances in Geomechanics, pp. 525–528. Taylor & Francis (2001)
12. Carstensen, C., Conti, S., Orlando, A.: Mixed analytical-numerical relaxation in finite single-slip crystal plastictiy. Continuum Mech. Thermodyn. **20**, 275–301 (2008). http://dx.doi.org/doi:10.1007/s00161-008-0082-0
13. Carstensen, C., Hackl, K., Mielke, A.: Nonconvex potentials and microstructures in finite-strain plasticity. Proc. R. Soc. Lond. A **458**, 299–317 (2002). http://dx.doi.org/doi:10.1098/rspa.2001.0864
14. Carstensen, C., Plecháč, P.: Numerical solution of the scalar double-well problem allowing microstructure. Math. Comp. **66**, 997–1026 (1997). http://dx.doi.org/doi:10.1090/S0025-5718-97-00849-1
15. Carstensen, C., Roubíček, T.: Numerical approximation of young measures in non-convex variational problems. Numer. Math. **84**, 395–415 (2000). http://dx.doi.org/doi:10.1007/s002119900122
16. Carstensen, C., Roubíček, T.: Numerical approximation of young measures in non-convex variational problems. Tech. Rep., 97–18 (1997). Universität Kiel
17. Chang, C.S., Hicher, P.Y.: An elasto-plastic model for grnaular materials with microstructural consideration. Int. J. Solids Struct. **42**, 4258–4277 (2005). http://dx.doi.org/doi:10.1016/j.ijsolstr.2004.09.021
18. Chang, C.S., Ma, L.: Elastic material constants for isotropic granular solids with particle rotation. Int. J. Solids Struct. **29**, 1001–1018 (1992). http://dx.doi.org/doi:10.1016/0020-7683(92)90071-Z
19. Chipot, M.: The appearance of microstructures in problems with incompatible wells and their numerical approach. Numer. Math. **83**, 325–352 (1999). http://dx.doi.org/doi:10.1007/s002110050452
20. Chipot, M., Collins, C.: Numerical approximation in variational problems with potential wells. SIAM J. Numer. Anal. **29**, 1002–1019 (1992). http://dx.doi.org/doi:10.1137/0729061
21. Collins, C., Kinderlehrer, D., Luskin, M.: Numerical approximation of the solution of a variational problem with a double well potential. SIAM J. Numer. Anal. **28**, 321–332 (1991). http://dx.doi.org/doi:10.1137/0728018
22. Conti, S., Hauret, P., Ortiz, M.: Conurrent multiscale computing of deformation microstructure by relaxation and local enrichment with application to single-crystal plasticity. Multiscale Model. Simul. **6**, 135–157 (2007). http://dx.doi.org/doi:10.1137/060662332
23. Conti, S., Ortiz, M.: Dislocation microstructures and the effective behavior of single crystals. Arch. Rational Mech. Anal. **176**, 103–147 (2005). http://dx.doi.org/doi:10.1007/s00205-004-0353-2
24. Conti, S., Theil, F.: Single-slip elastoplastic microstructures. Arch. Ration. Mech. Anal. **178**, 125–148 (2005). http://dx.doi.org/doi:10.1007/s00205-005-0371-8
25. Dacorogna, B.: Direct Methods in the Calculus of Variations. Springer, Berlin-Heidelberg-New York (1989)

26. Dacorogna, B.: Necessary and sufficient conditions for strong ellipticity of isotropic functions in any dimension. Discrete Contin. Dyn. Syst. B. **1**, 257–263 (2001). http://dx.doi.org/doi:10.3934/dcdsb.2001.1.257
27. de Borst, R.: Simulation of strain localization: a reappraisal of the Cosserat-continuum. Eng. Comp. **8**, 317–332 (1991). http://dx.doi.org/doi:10.1108/eb023842
28. DeSimone, A., Dolzmann, G.: Macroscopic response of nematic elastomers via relaxation of a class of SO(3)-invariant energies. Arch. Ration. Mech. Anal. **161**, 181–204 (2002). http://dx.doi.org/doi:10.107/s002050100174
29. Dolzmann, G., Walkington, N.J.: Estimates for numerical approximations of rank one convex envelopes. Numer. Math. **85**, 647–663 (2000). http://dx.doi.org/doi:10.1007/PL00005395
30. Le Dret, H., Raoult, A.: The quasiconvex envelope of the Saint Venant-Kirchhoff stored energy function. Proc. Roy. Soc. Edinburgh **125A**, 1179–1192 (1995). http://dx.doi.org/doi:10.1017/S0308210500030456
31. Ehlers, W., Volk, W.: On shear band localization phenomena of liquid-saturated granular elastoplastic porous solid materials accounting for fluid viscosity and micropolar solid rotations. Mech. Cohes.-Frict. Mat. **2**, 301–320 (1997). http://dx.doi.org/doi:10.1002/(SICI)1099-1484(199710)2:4<301::AID-CFM34>3.0.CO;2-D(10.1002/(SICI)1099-1484(199710)2:4<301::AID-CFM34>3.0.CO;2-D)
32. Govindjee, S., Hackl, K., Heinen, R.: An upper bound to the free energy of mixing by twin-compatible lamination for n-variant martensitic phase transformations. Continuum Mech. Thermodynam. **18**, 443–453 (2007). http://dx.doi.org/doi:10.1007/s00161-006-0038-1(10.1007/s00161-006-0038-1)
33. Gudehus, G., Nübel, K.: Evolution of shear bands in sand. Géotechnique **54**, 187–201 (2004). http://dx.doi.org/doi:10.1680/geot.2004.54.3.187(10.1680/geot.2004.54.3.187)
34. Gürses, E., Miehe, C.: On evolving deformation microstructures in non-convex partially damaged solids. J. Mech. Phys. Solids **59**, 1268–1290 (2011). http://dx.doi.org/doi:10.1016/j.jmps.2011.01.002(10.1016/j.jmps.2011.01.002)
35. Hackl, K., Heinen, R.: An upper bound to the free energy of n-variant polycrystalline shape memory alloys. J. Mech. Phys. Solids. **56**, 2832–2843 (2008). http://dx.doi.org/doi:10.1016/j.jmps.2008.04.005(10.1016/j.jmps.2008.04.005)
36. Kohn, R.V.: The relaxation of a double-well energy. Continum Mech. Thermodynam. **3**, 193–236 (1991). http://dx.doi.org/doi:10.1007/BF01135336
37. Kohn, R.V., Strang, G.: Optimal design and relaxation of variational problems I. Comm. Pure Appl. Math. **39**, 113–137 (1986). http://dx.doi.org/doi:10.1002/cpa.3160390107
38. Kohn, R.V., Strang, G.: Optimal design and relaxation of variational problems II. Comm. Pure Appl. Math. **39**, 139–182 (1986). http://dx.doi.org/doi:10.1002/cpa.3160390202
39. Kohn, R.V., Vogelius, M.: Relaxation of a variational method for impedance computed tomography. Comm. Pure Appl. Math. **40**, 745–777 (1987). http://dx.doi.org/doi:10.1002/cpa.3160400605
40. Lambrecht, M., Miehe, C., Dettmar, J.: Energy relaxation of non-convex incremental stress potentials in a strain-softening elastic-plastic bar. Int. J. Soids Struct. **40**, 1369–1391 (2003). http://dx.doi.org/doi:10.1016/S0020-7683(02)00658-3
41. Morrey, C.B.: Quasi-convextiy and the lower seimicontinuity of multiple integrals. Pac. J. Math. **2**, 25–53 (1952). See http://projecteuclid.org/euclid.pjm/1103051941http://projecteuclid.org/euclid.pjm/1103051941
42. Nicolaides, R.A., Walkington, N.J.: Computation of microsturcture utilizing Young measures representations. In: Rogers, C.A., Rogers, R.A. (eds.) Recent Advances in Adaptive and Sensory Materials and their Applications, pp. 131–141.Technomic Publ., Lancaster (1992)
43. Nicolaides, R.A., Walkington, N.J.: Strong convergence of numerical solutions to degenrate variational problems. Math. Comp. **64**, 117–127 (1992). See http://www.jstor.org/stable/2153325http://www.jstor.org/stable/2153325
44. Oda, M., Kazama, H.: Microstructure of shear bands and its relation to the mechanisms of dilatancy and failure of dense granular soils. Géotechnique **48**, 465–481 (1998). http://dx.doi.org/doi:10.1680/geot.1998.48.4.465

45. Papanicolopulos, S.A., Veveakis, E.: Sliding and rolling dissipation in Cosserat plasticity. Granular Matter **13**, 197–204 (2011). http://dx.doi.org/doi:10.1007/s10035-011-0253-8
46. Pasternak, E., Mühlhaus, H.B.: Cosserat continuum modelling of granulate materials. In: Valliappan, S., Khalili, N. (eds.) Computational Mechanics - New Frontiers for New Millennium, pp. 1189–1194. Elsevier Science (2001)
47. Pedregal, P.: Parametrized Measures and Variational Principles. Birkhäuser (1997)
48. Pedregal, P.: Numerical approximation of parametrized measures. Numer. Funct. Anal. Optim. **16**, 1049–1066 (1995). http://dx.doi.org/doi:10.1080/01630569508816659
49. Pedregal, P.: On numerical analysis of non-convex variational problems. Numer. Math. **74**, 325–336 (1996). http://dx.doi.org/doi:10.1007/s002110050219
50. Raoult, A.: Quasiconvex envelopes in nonlinear elasticity. In: Schröder, J., Neff, P. (ed.) Poly-, Quasi- and Rank-One Convexity in Applied Mechanics, pp. 17–51. Springer, Vienna (2010). http://dx.doi.org/doi:10.1007/978-3-7091-0174-2
51. Roubíček, T.: Relaxation in Optimization Theory and Variational Calculus. Valter de Gruyter, Berlin, New York (1997)
52. Roubíček, T.: Finite element approximation of a microstructure evolution. Math. Methods Appl. Sci. **17**, 377–393 (1994). http://dx.doi.org/doi:10.1002/mma.1670170505
53. Roubíček, T.: Numerical approximation of relaxed variational problems. J. Convex Anal. **3**, 329–347 (1996). See http://eudml.org/doc/i33027http://eudml.org/doc/233027
54. Sawada, K., Zhang, F., Yashima, A.: Rotation of granular material in laboratory tests and its numerical simulation using TIJ-Cosserat continuum theory. Comput. Methods, 1701–1706 (2006). http://dx.doi.org/doi:10.1007/978-1-4020-3953-9_104
55. Suiker, A.S.J., de Borst, R., Chang, C.S.: Micro-mechanical modelling of granular material. Part 1: Derivation of a second-gradient micro-polar constitutive theory. Acta Mechanica **149**, 161–180 (2001). http://dx.doi.org/doi:10.1007/BF01261670
56. Suiker, A.S.J., de Borst, R., Chang, C.S.: Micro-mechanical modelling of granular material. Part 2: Plane wave propagation in infinite media. Acta Mechanica **149**, 181–200 (2001). http://dx.doi.org/doi:10.1007/BF01261671
57. Tejchman, J., Niemunis, A.: FE-studies on shear localization in an anisotropic micro-polar hypoplastic granular material. Granular Matter. **8**, 205–220 (2006). http://dx.doi.org/doi:10.1007/s10035-006-0009-z
58. Tordesillas, A., Peters, J.F., Muthuswamy, M.: Role of particle rotations and rolling resistance in a semi-infinite particulate solid indented by a rigid flat punch. ANZIAM J. **46**, C260–C275 (2005)
59. Tordesillas, A., Walsh, S.D.C.: Incorporating rolling resistance and contact anisotropy in micromechanical models of granular media. Powder Technol. **124**, 106–111 (2002). http://dx.doi.org/doi:10.1016/S0032-5910(01)00490-9
60. Tordesillas, A., Walsh, S.D.C., Gardiner, B.: Bridging the length scales: Micromechanics of granular media. BIT Numer. Maths. **44**, 539–556 (2004). http://dx.doi.org/doi:10.1023/B:BITN.0000046817.60322.ed
61. Trinh, B.T., Hackl, K.: Performance of mixed and enhanced finite elements for strain localization in hypoplasticity. Int. J. Numer. Anal. Methods Geomech. **35**, 1125–1150 (2012). https://doi.org/10.1002/nag.1042
62. Trinh, B.T., Hackl, K.: Modelling of shear localization in solids by means of energy relaxation. Asia Pac. J. Comput. Eng. **1**, 1–21 (2014)
63. Trinh, B.T., Hackl, K.: A model for high temperature creep of single crystal superalloys based on nonlocal damage and viscoplastic material behavior. Contin. Mech. Thermodyn. **26**, 551–562 (2014)
64. Young, L.C.: Generalized Curves and the Existence of an Attained Absolute Minimum in the Calculus of Variations, pp. 212–234 (1937)